JETIR.ORG

ISSN: 2349-5162 | ESTD Year: 2014 | Monthly Issue

# JOURNAL OF EMERGING TECHNOLOGIES AND INNOVATIVE RESEARCH (JETIR)

An International Scholarly Open Access, Peer-reviewed, Refereed Journal

# Correlation of Anti-cancer activity and DNA binding affinity of novel Ru(II) Polypyridyl complex – A Biophysical study

Sravani Gudikandula<sup>1</sup>, Navaneetha Nambigari<sup>1,2\*</sup>

- 1. Department of Chemistry, University College of Science, Saifabad, Osmania University, Hyderabad -500 004, Telangana State, INDIA.
- 2. Department of Chemistry, University College of Science, Osmania University, Tarnaka, Hyderabad 500007, Telangana State, INDIA.

#### **Abstract**:

A Ruthenium(II) polypyridyl complex of the type  $[Ru(NN)_2L]$ where NN=phen,1,10 Phenanthroline and Intercalator ligand L=TMPIP=2-(3,4,5-Trimethoxy-phenyl)-H-imidazole[4,5-f][1,10]phenanthroline were synthesized and characterized by spectroscopic techniques like IR,  $^1H$  NMR,  $^{13}C$  NMR, Mass, UV and Elemental analysis. The DNA binding affinity of metal complex were investigated by using Biophysical methods-Electronic absorption titration, Fluorescence emission titration and viscosity studies. The absorption and fluorescence binding constant  $(K_b)$  of complex with CT DNA is  $1.5 \times 10^5$  and  $2.1 \times 10^6$  M $^{-1}$  respectively. The data is comparable with the standard DNA metallointercalator due to the added planarity of the phenanthroline ligand and also the viscosity study reveal an intercalative mode of binding. In photocleavage studies the complexes successfully cleaved the pBR322 DNA.MTT assay of the complex reveal good anticancer activity against MCF-7 Cell line is  $IC_{50} = 17.42 \pm 0.29 \mu g/ml$  indicating a correlation with DNA binding affinity.

**Key words**: Polypyridyl, Biophysical, DNA binding, photo cleavage, anticancer activity.

# 1. Introduction

Bioinorganic chemistry is a rapidly developing area of fascinating opportunities and creativity (Guang-Bin Jiang, 2020). The primary issue under investigation in this area is development of new drugs with DNA-binding properties, bind to DNA by intercalation, covalent, electrostatic, and groove binding. According to recent research, transition metal complexes are crucial for understanding DNA interaction and photocleavage. The effective anti-cancer medication cis-platin was discovered as a result of the diverse applications of transition metal complexes in biochemistry, including the use of particular binding agents and foot printing research. The results of its use led to the development of innovative metal-based anti-cancer medications that are safe for healthy cells while precisely targeting cancer cells (Nataro, 2017; Hu, 2017).

In cancer therapy metal complexes have garnered a lot of fascination because of the clinical effects of cisplatin and its derivatives (Kelland, 1999). Furthermore, Pt medications can cause major adverse side effects such as nephrotoxicity, ototoxicity and so on which limit their efficacy (Oun, 2018). The development of innovative anti-cancer medications, Ru complexes have been offered as a complement to Pt complexes (Kuhn, 2015). Ru complexes have grown to be widely used in DNA investigating, cellular image processing, protein monitoring, and anticancer activity because of their distinctive photophysical characteristics (Lentz, 2009). In addition to being rapidly eliminated in vivo and readily absorbed by tumor tissues, ruthenium and its complexes are also low in toxicity and have promising anticancer application possibilities. In order to control cell pathways and trigger tumor cell apoptosis, the ruthenium complexes can be employed as particular inhibitors for telomerase, DNA topoisomerase, protein kinase, and other enzymes (Yulin, 2018).

According to structure-activity correlation studies, Ru complexes could suppress tumor cells through processes similar to cisplatin (Novakova, 2005). The frontier molecular orbital theory states that the HOMO (highest occupied molecular orbital), LUMO (lowest unoccupied molecular orbital) and related orbitals have a significant impact on the electronic properties of chemical compounds. In general, electrons are donors in HOMO orbitals and acceptors in LUMO orbitals. The energy difference between the HOMO and LUMO also acts as a chemical activity barometer for the molecule (Morrall, 2006).

Many Ru complexes are now undergoing phase I or II clinical studies (Jabłońska, 2013; Strasser, 2015). They have distinct optical and electrochemical properties with a prominent absorption band in the visible light spectrum, owing to metal-to-ligand charge transfer (MLCT) (Norden, 1996). Introduction of substitutions in the polypyridyl ligands may lead to different electronic characteristics, the MLCT absorption band, emission wavelength, and emission lifetime may be easily modified. Significant research has also established that polypyridyl Ruthenium(II) complexes are promising chemotherapeutic medicines that can attach to numerous nucleic acid sequences in various mechanisms, such as insertion and groove cross-binding (Metcalfe, 2003; Luedtke, 2003).NAMIA, KP1019, and KP1330 are currently in phase II clinical testing (Ang, 2011). The photocleavage studies of these complexes with pBR322 DNA, cytotoxic studies against to the specific selected cell lines shows that all the complexes demonstrated effective activity in a dose-dependent manner (Schatzschneider, 2008; Tan, 2008; Puckett, 2008).

In the current study, the synthesis of ligand 3,4,5 TMPIP[2-(3,4,5-Trimethoxy-phenyl)-H-imidazole[4,5-f][1,10]phenanthroline] and its metal complexes and Characterization of the complexes were achieved by IR, UV, H NMR, MASS and Elemental analysis. The binding correlations of CT-DNA to these complexes were investigated by using UV-Visible absorption titration, Fluorescence emission &viscosity experiment.

#### 2. Experimental

Except where otherwise noted, all analytical grade reagents and solvents were used exactly as they were supplied. The following substances were purchased from Merck: 1,10-phenanthroline monohydrate (phen), 2,2'-bipyridine (bpy), 4,4'-dimethyl2,2'-bipyridine (dmb), and 4,4'-dimethyl-1,10 ortho phenanthroline (dmp). Super coiled pBR322 plasmid DNA (stored at 20°C) and calf thymus DNA (CT-DNA) were obtained from Fermentas Life Sciences and Aldrich, respectively, and used in their original forms. From Genei, agarrose gel was purchased. All studies used 18.2mX ultrapure Milli-Q water. In tris (hydroxymethyl) amino methane, Tris-HCl buffer (5 m.mol. TrisHCl, 50 mM NaCl, pH 7.2), the binding affinity of the metal complex for CT-DNA was estimated. AT absorbances of 260 and 280 nm and a concentration of DNA per nucleotide at a molar extinction of 6600 M<sup>-1</sup> cm<sup>-1</sup> protein-free DNA could be seen using spectrophotometry (Steck, 1943). Stock solutions of metal complexes were prepared in the DMSO solvent and kept at 40°c, used in less than 5 days. All the stock solutions were diluted further for required concentration in buffer.

The Shimadzu UV-2600 spectrophotometer was used to record the UV-Vis spectra. The Cary Eclipse instrument serial number (MY12400004) Spectrofluorometer was used to record the luminescence spectral data needed to calculate the binding constants. Using KBr disks, IR spectra were recorded using a PerkinElmer 1605 Fourier transform IR spectrometer. With tetramethylsilane serving as the internal standard and dimethyl-d<sub>6</sub> sulfoxide (DMSO-d<sub>6</sub>) serving as the solvent, <sup>1</sup>H and <sup>13</sup>C NMR spectra were captured using a Bruker 400-MHz spectrometer. The PerkinElmer 240 elemental analyzer was used to do elemental microanalysis on the elements C, H, and N. A Quattro LC triple quadrupole mass spectrometer equipped with the Mass Lynx software (Micro mass, Manchester, UK) 3 was used to record the mass spectra.

**2.1. Synthesis& characterization of ligand and metal complexes:** 1,10 phenanthroline-5,6-dione and [Ru(NN)<sub>2</sub>Cl<sub>2</sub>], starting materials were synthesized according to the standard procedure where NN= phen (Yamada, 1992; Sullivan, 1978). Synthetic route for ligand, complexes were shown in scheme-1.

# 2.1.1.Synthesis of 3,4,5 TMPIP (2-(3,4,5-Trimethoxy phenyl)-1H-imidazole[4,5-f] [1,10] phenanthroline)(L):

Novel ligand 3,4,5 TMPIP was synthesized according to the literature (Zheng, 2010).1,10-Phenanthroline5,6-dione(0.53g,2.50mM), 3,4,5 - Trimethoxy benzaldehyde (0.686g,3.50mM), ammonium acetate (3.88 g, 50.0mM) were dissolved in glacial acetic acid (15ml) and refluxed together for 4-5 hours (Scheme 1). The resultant solution was cooled to room temperature and diluted with  $H_2O$ , and then drop wise addition of concentrated aqueous Ammonia yields a yellow compound, which was collected and washed with  $H_2O$ . This compound was recrystallized with  $C_5H_5N.H_2O$  and dried. (Yield: 62%).

Scheme-1: Synthetic route for the preparation of ligand and structures of ruthenium (II) Complexes

# Analytical data:

 $C_{22}H_{18}N_4O_3: cal. C, 68.38; H, 4.58; N, 13.75; found: C, 68.27; H, 4.37; N, 13.45. ES^+-MS Calc: 386.40; found: 387.14[M+H]^+, 1 MMR (DMSO-d6, 400 MHz): <math>\delta 1.9(s, 1H), \delta 2.5(t, 1H), \delta 3.3(s, 1H), \delta 3.7(s, 2H), \delta 3.9(s, 3H), \delta 7.6(s, 1H), \delta 7.8(q, 1H), \delta 8.9(d, 1H), \delta 9.0(d, 1H). 1^3C[ ^1H]NMR(100MHz, DMSO-d_6, d, ppm) : 157.24, 153.08, 151.95, 140.05, 138.45, 128.37, 124.94, 104.72, 60.74, 56.81, 40.60& IR (KBr, cm^-): 3,402 (v, N-H), 1246 (v, C-N), 1131 (v, C-O-C)$ 

## 2.1.2. Synthesis of [Ru(phen)<sub>2</sub>Cl<sub>2</sub>(TMPIP)](ClO<sub>4</sub>)<sub>2</sub>.2H<sub>2</sub>O

This complex was synthesized by using the above procedure in which [Ru (phen)<sub>2</sub>Cl<sub>2</sub>] 2H<sub>2</sub>O (0.284 g,0.5 mM) and TMPIP(0.193 g,0.5 mM) were mixed in a mixture of ethanol (25 ml) and water (15 ml), and refluxed for 8 h at 120°C under inert N<sub>2</sub> atmosphere. When the light purple color solution was achieved, it is cooled to room temperature and an equivalent quantity of saturated aqueous NaClO<sub>4</sub> solution was introduced under brisk stirring. An orange yellow precipitate was collected and washed with small amounts of water, ethanol and diethyl ether, then dried under vacuum (yield:72.94%) (Goss, 1985)

**Analytical data:**RuC<sub>46</sub>H<sub>34</sub>N<sub>8</sub>O<sub>3</sub>; cal. C,63.38; H,4.58; N, 13.75; found: C, 63.26; H,4.34; N, 13.12.ES<sup>+</sup>-MS Calc: 423.94 ; found:  $424 \text{ [M+H]}^+$ ,  $^1\text{H} \text{ NMR} \text{ (DMSO-d6, 400 MHz):} \delta 7.6 (d,1H), 7.7 (t,2H), 8.0 (d,1H), 8.1 (d,1H), 8.3 (d,2H), 8.7 (d,2H0, 1.5 (d,1H), 1.5 (d,2H0, 1.5 (d,2H0,$ 

8.9(d,1H), 9.0(d,1H), 3.7(s,1H) 3.9(s,3H), 13.6(s,1H), 14.2(s,1H),  $^{13}C[^{1}H]$  NMR (100 MHz, DMSO-d<sub>6</sub>, d, ppm):166.44, 156.06,147.92,138.54, 128.73,124.94,113.05, 105.70, 76.39, 72.51, 62.34, 55.67, 50.73, 45.06, 30.30, 24.96, 21.51, 17.70, 13.24,9.46& IR (KBr, cm<sup>-1</sup>): 3,598(v, N-H),1237 (v, C-N), 1073(v, C-O-C), 622(v<sub>Ru-N</sub>).

## 2.2. DNA binding studies

The techniques employed in our procedures to determine the binding affinity for the Ruthenium (II) polypyridyl complex are the main topics of this section which were discussed in our protocols (Navaneetha, 2022).

## 2.2.1. Electronic absorption studies

The tris(hydroxymethyl)-aminomethane (Tris,5 mM), sodium chloride (50 mM), and hydrochloric acid were added to double-distilled water to create the proper pH balance for the experiments comprising the interaction of the ruthenium (II) complexes with CT-DNA. The ratio of UV absorbance from a solution of CT-DNA in the buffer was roughly 1.9 at 260 and 280 nm, demonstrating that the DNA was adequately free of protein. Using the molar extinction coefficient value of  $6600 \text{ dm}^3 \text{ mol}^{-1}$  cm<sup>-1</sup> at 260 nm, absorption spectroscopy was used to calculate the DNA concentration per nucleotide. The nucleotide concentration was varied from 10 to  $100\mu\text{M}$  while the complex concentration was kept constant ( $20\mu\text{M}$ ) for the electronic absorption titration studies. Equal quantities of DNA were used to measure the absorption spectra (Novakova, 2005; Puckett, 2008).

$$[DNA]/\left(\epsilon_{a}-\epsilon_{f}\right)=[DNA]/\left(\epsilon_{b}-\epsilon_{f}\right)+1/\left.K_{b}\left(\epsilon_{b}-\epsilon_{f}\right)\right] \tag{1}$$

The apparent absorption coefficients  $\epsilon_a$ ,  $\epsilon_f$ , and  $\epsilon_b$  equate to  $A_{obsd}/[complex]$ , the extinction coefficient of the compound while it is free, and the extinction coefficient of the compound when it is fully bound to DNA, respectively, where [DNA] is the concentration of DNA in base pairs.  $K_b$  is determined by plotting [DNA]/( $\epsilon_a$ - $\epsilon_f$ ) versus [DNA] and  $K_b$  calculated using the slope to intercept ratio as shown in equation 1.

#### 2.2.2. Fluorescence emission studies

The previously described approach was used to perform the emission titrations. In this titrations, the metal complex concentration was maintained at an optimal level while raising the DNA concentration to record the spectra; these emission values fell between 550 and 750 nm. The formula used to determine the binding constant was (Ravi Kumar, 2020).

$$C_b = C_t[(F - F_0 / F_{max} - F_0)]$$
 (2)

Where  $C_t$  is the total complex concentration, F is the observed fluorescence emission intensity at a given DNA concentration,  $F_0$  is the emission intensity in the absence of DNA, and  $F_{max}$  is the time when the complex is maximally bound to DNA. A graph was created between the  $r/C_f$  vs r, binding constant, where r is the  $C_b/[DNA]$  and  $C_f$  is the concentration of the free complex, using the Scatchard equation 2 to compute the binding constant.

# 2.2.3. Viscosity Experiment

Utilizing an Ostwald's viscometer kept in a thermostatic bath at a constant temperature of  $29 \pm 0.1^{\circ}c$ , viscosity measurements were taken. Each sample's flow time was measured three times using a digital stopwatch, and the average flow time was computed. Data are displayed as  $(\eta/\eta_0)^{1/3}$  vs binding ratio (Tan, 2008), where  $\eta$  is the DNA's viscosity when the complex is present and  $\eta_0$  is the DNA's viscosity when CT-DNA is used alone. The measured flow time of DNA-containing solutions (t) was used to determine the viscosity values, which were then adjusted for the observed flow time of the buffer alone  $(t_0)$ .

# 2.2.4. Quenching studies

The Tris - HCl buffer solution (pH = 7.5) was employed in the fluorescence experiments. Different concentrations of the complexes (1, 2, 3, and 4) were added to an ethidium bromide and CT-DNA solution to allow for reaction. The concentration of the complexes was kept between 10 and 100  $\mu$ M, whereas ethidium bromide and CT-DNA were kept at 130 and 40  $\mu$ M, respectively. Ethidium bromide's emission range was kept between 560 and 760 nm, and its emission spectra was observed at 520 nm. By using the Stern-Volmer equation:  $I_0/I = 1 + K_{SV} r$ , where I and  $I_0$  stand for fluorescence intensities in the presence and absence of complexes, respectively, and  $K_{SV}$  linear Stern-Volmer quenching constant based on the ratio of  $r_{EB}$  (the ratio of the bound concentration of EB to the concentration of DNA) and total concentration of the complex to that of DNA is r, thus the Spectra were examined (Zhang, 2016; Mariappan, 2018).

#### 2.2.5. DNA cleavage experiment

By using the agarose gel electrophoresis method, the metal complexes capacity to cleave DNA through photolytic investigations was calculated. In this test, metal complexes were applied to supercoiled pBR322 DNA at several quantities, and then the DNA was diluted with TrisHCl buffer at pH 7.2. The pretreatment DNA-sample system was mixed with bromophenol blue (2 L) and then incubated for a further two hours at 37°C. The samples were then loaded onto the wells of a 1% agarose gel that was set in a tray containing TAE buffer (pH 8.0) and electrophoresed for 45 minutes at 70 V. Before electrophoresis, the gel was treated with ethidium bromide. With the use of a BIO-RAD Gel documentation system, bands were seen under an ultraviolet (UV) transilluminator and the gel that resulted was photographed (Aveli, 2021).

#### 2.3. Cytotoxicity

The cells were seeded in a 96-well flat-bottom microplate and maintained at 37°C in 95% humidity and 5% CO2 overnight. Different concentration (100, 50, 25, 12.5, 6.25, 3.125  $\mu$ g/ml) of samples were treated. The cells were incubated for another 48 hours. The wells were washed twice with PBS and 20  $\mu$ L of the MTT staining solution was added to each well and the plate was incubated at 37°C. After 4h, 100  $\mu$ L of DMSO was added to each well to dissolve the formazan crystals, and absorbance was recorded with a 570 nm using microplate reader (Ravi Kumar, 2020).

**Formula**: Surviving cells (%) = Mean OD of test compound /Mean OD of Negative control  $\times 100$  Using graph Pad Prism Version5.1, we calculate the IC<sub>50</sub> of compounds.

#### 3. Results and discussion

# 3.1. Synthesis and Characterization

Synthesis of the novel complex is confirmed by CHN analysis, Mass,  $^{1}H$  NMR,  $^{13}C$  NMR, FTIR &Absorption spectrum. IR spectrum shown bands at 3402 (v, N-H), 1246 (v, C-N), 1131 (v, C-O-C) after complex formation the bands further shifted to 3,598(v, N-H),1237 (v, C-N), 1073 (v, C-O-C). The new band at 622 CM<sup>-1</sup> appeared in the complex which is due to the formation of metal -nitrogen bond ( $v_{Ru-N}$ ) confirms the complex formation (Figure 1-2). H NMR spectra show the ligand characteristic aliphatic peaks at  $\delta$  3.97 to 1.91 ppm, these protons were shifted to around  $\delta \sim 4.0$  to 2.50 ppm after complex formation (Figure 2-4). In the complex, the N- H proton appeared around 14 ppm,  $^{13}C$ Spectra of the complexes show shift in the chemical shift values compared to ligand, confirming the complex formation ((Figure 5-6).). M/Z values from the mass correlates with theoretical value ((Figure 7 - 8). The MLCT band in absorption spectrum for the complex appeared at 420 nm which is not shown by ligand, confirming complex formation (Figure 9, Table-1).

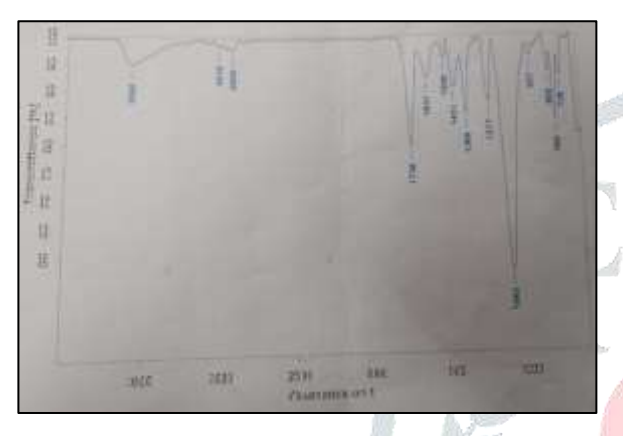
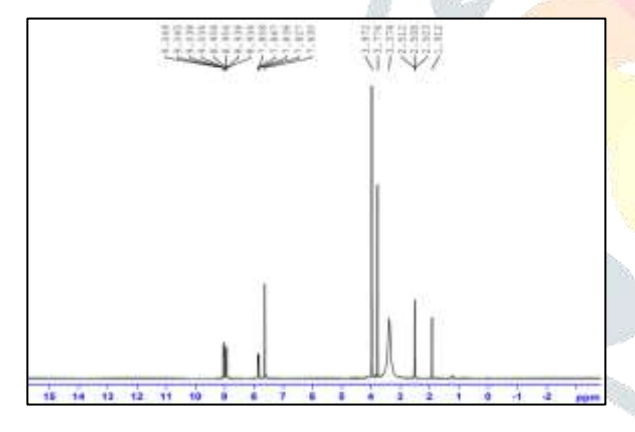


Fig. 1. IR Spectra of Intercalator, Ligand TMPIP

Fig. 2. IR Spectra of [Ru(phen)<sub>2</sub> TMPIP]<sup>2+</sup>



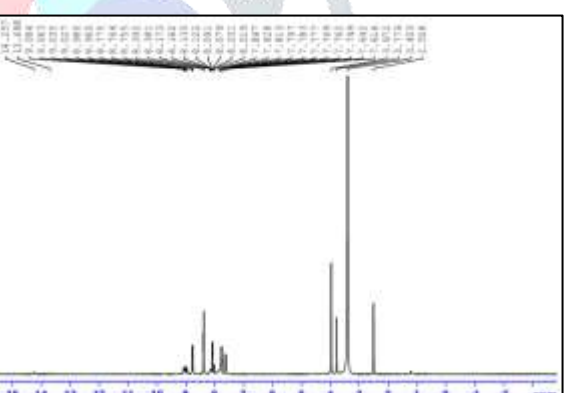
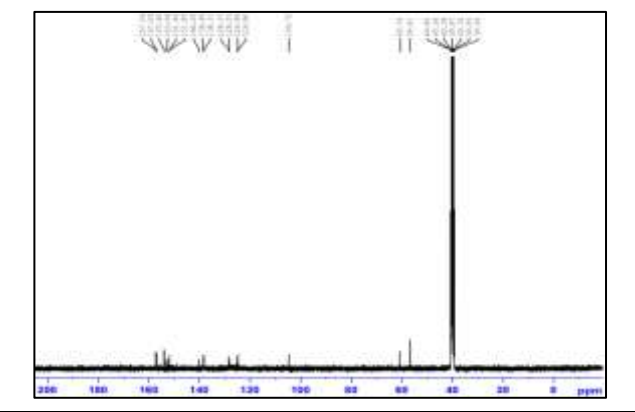


Fig. 3. <sup>1</sup>H NMR Spectra of Intercalator, Ligand TMPIP

Fig.4. <sup>1</sup>H NMR Spectra of [Ru(phen)<sub>2</sub> TMPIP]<sup>2+</sup>



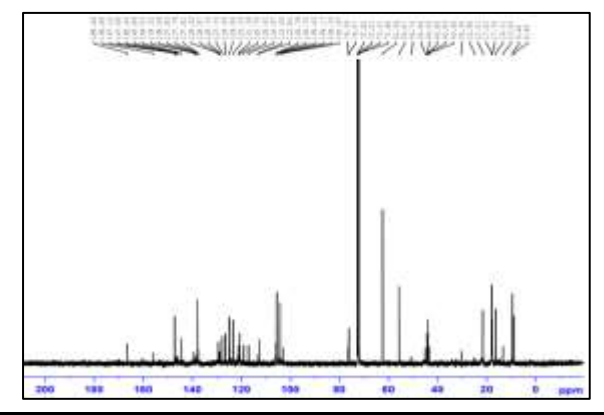


Fig.5. <sup>13</sup>C NMR Spectra of Intercalator, LigandTMPIP

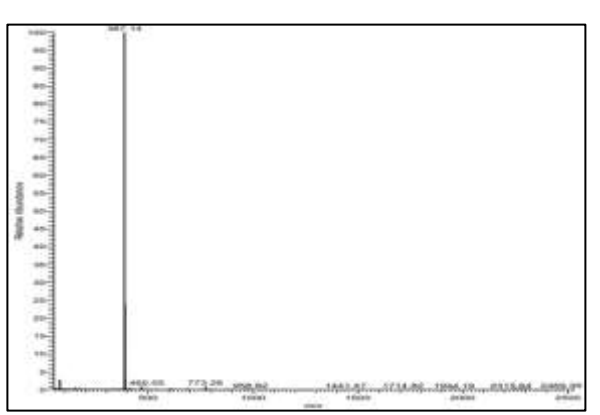


Fig.7. Mass Spectra of Intercalator, Ligand TMPIP

# Fig.6. <sup>13</sup>C NMR Spectra of [Ru(phen)<sub>2</sub> TMPIP]<sup>2+</sup>

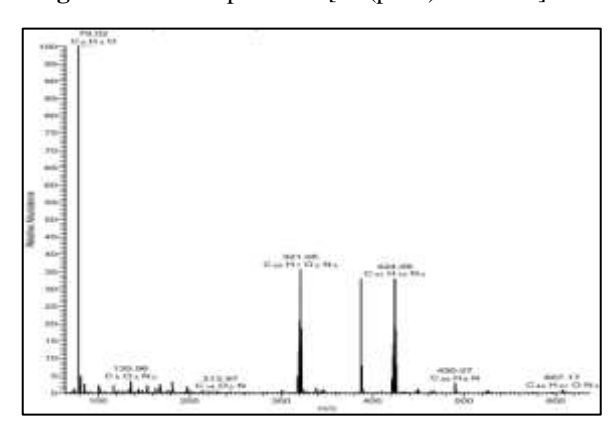


Fig.8.Mass Spectra of [Ru(phen)<sub>2</sub> TMPIP]<sup>2+</sup>

# 3.2. DNA Binding Studies

#### 3.2.1. UV-Visible absorption Studies

The UV Visible spectra of complex show characteristic MLCT transition in the visible region. Binding affinity of metal complexes to CT-DNA can be characterized by Hypochromism and bathochromism in MLCT band. Electronic absorption titration was performed in the presence and absence of DNA were shown in the Figure 9.

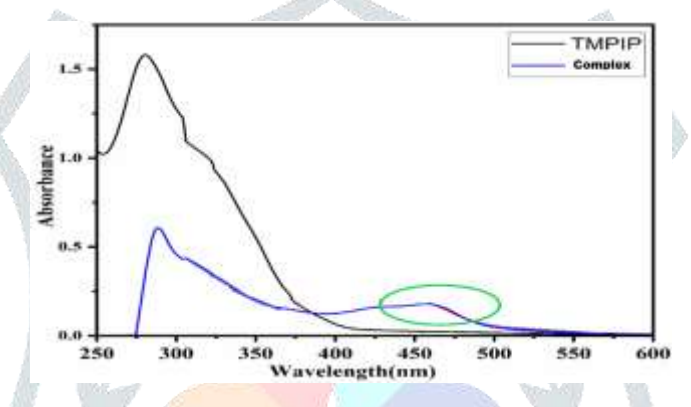


Fig. 9. Electronic absorption spectra of TMPIP and its complex

Table.1 Electronic spectral data of TMPIP& its complexes

Ligand/Ru(II) complex	Absorption region, Amax	Band assigned
TMPIP	270	$\pi \rightarrow \pi^* (INCT)$
[Ru(phen)2TMPIP]2+	275	$\pi{ ightarrow}\pi^*$
	420	(MLCT)

The metal complex concentration kept constant, to this increased concentrations of CT-DNA added. By the addition of increased amounts of DNA decrease in the absorption observed in the MLCT band region at 420 nm respectively. Hypochromic shift of 19.03% and bathochromismof4nm of complexes. Hypochromism shift results due to strong p-p stocking interaction between intercalated aromatic chromophore of metal complex and base pair units of DNA. Bathochromism results due to coupling of antibonding p orbital's of intercalated metal complex with bonding p orbitals of DNA base pairs which leads to a decrease in p-p\* transition energy.  $\pi$ -  $\pi$  interactions between the metal complex aromatic chromophore and the DNA base pair units leads to hypochromism. The interaction of anti-bonding orbitals ( $\pi$ ) of intercalated metal complex with bonding ( $\pi$ ) orbitals of DNA leads to bathochromism. Figure 1 show the UV-Visible Absorption spectra of complex in the presence (lower) and in the absence (top) of CT-DNA in Tris–HCl buffer. The titration of the metal complex solution (constant  $10~\mu$ M of 0.001M concentration) in Tris–HCl buffer in the cuvette, and 0– $120~\mu$ L of DNA (stock concentration =  $0.617 \times 10^{-4}$  M) is added to the buffer solution. The intrinsic binding constant Values for the complexes  $1.5 \times 10^5$  respectively (Table.1). The complex has shown good binding results, owing to more planarity of ancillary ligand phen.

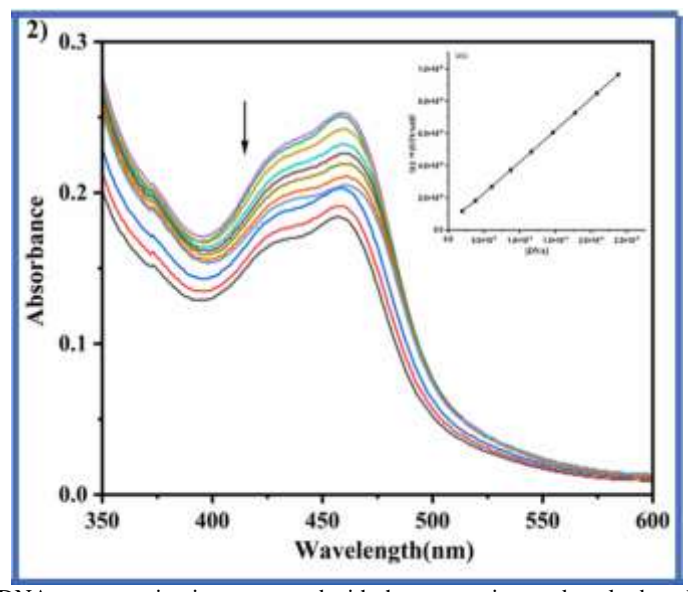
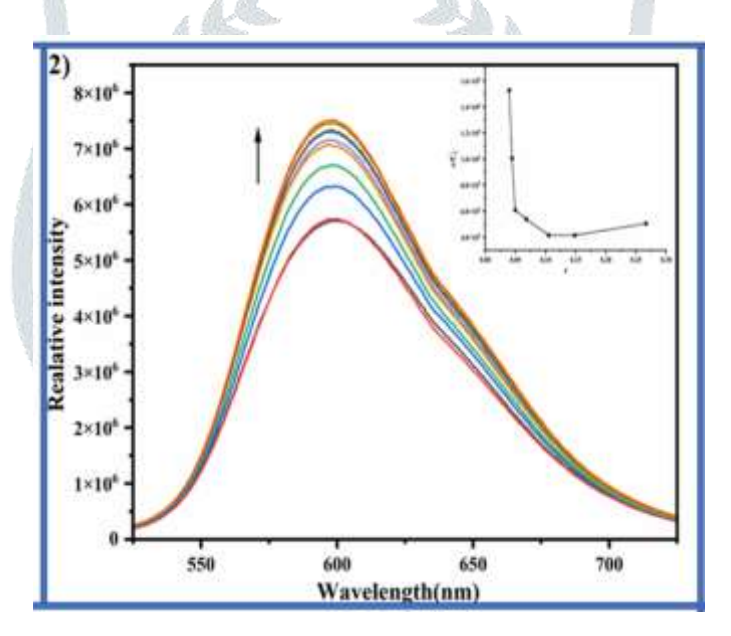


Fig.1. Changes upon increase of  $\overline{DNA}$  concentration is represented with the arrows, inserted a plot by taking  $[DNA]/(\epsilon a - \epsilon f)$  Vs [DNA] for the titration of DNA with Ru(II) polypyridyl complex which gives intrinsic binding constant  $(K_b)$  further.

#### 3.2.2. Fluorescence emission studies:

The binding strength of metal complex to CT-DNA further assessed by Fluorescence emission titrations. The complex excited at 420 nm then strong emission observed at 605nm band regions respectively. While increasing the concentration of CT-DNA change in the emission intensity of the complexes are shown in the figure. 2. The complexes emission intensities gradually rise with increasing DNA concentration until they reach a steady level. The modified Scatchard equation used for the calculation of intrinsic binding constant ( $K_b$ ) from emission data. Binding constants ( $K_b$ ) were obtained from Scatchard plots where  $r/C_f$  vs r is plotted. Where  $C_f$  is free ligand concentration, r is the binding ratio  $C_b/[DNA]$ . The  $K_b$  values for the complex is  $2.1 \times 10^6$ . The values obtained from absorption and emission titrations were in accordance with each other.



 $\begin{tabular}{ll} Fig. 2. The Ruthenium (II) complex emission spectra in Tris-HCl buffer. Upon the addition of CT-DNA; the arrow shows the intensity change by increasing DNA concentration. inset: Scatchard plot of the complexes , from which binding constant ($K_b$) calculated. \end{tabular}$ 

Table 2. Absorption, emission, and quenching binding constants of ruthenium (II) complexes with CT-DNA.

Complex	K <sub>b</sub> (M <sup>-1</sup> ) (Absorption)	K <sub>b</sub> (M <sup>-1</sup> ) (Emission)	K <sub>sv</sub> value
[Ru(phen)2(qpd)]+2	$1.5 \times 10^5$	$2.1 \times 10^6$	1.65 x10 <sup>4</sup>

#### 3.2.3. Quenching studies

It has been shown that DNA groove binders and intercalator can both diminish the fluorescence intensity. However, the reduction caused by groove binders is only minor, whereas the replacement of Ethidium Bromide (EB) by intercalator can result in a considerable reduction in intensity. Further fluorescence investigations using the quenching method were used to determine the intercalative mode of complex binding to CT-DNA. This experiment was performed by taking a well-known intercalating agent Ethidium bromide. When EB intercalate with DNA, there is a dramatic increase in emission intensity. This represents the way that EB interacts with DNA base pair units. In the current study, the solution of Ethidium bromide [40  $\mu$ M] and CT-DNA [130 $\mu$ M] increased amount of complex [10-100 $\mu$ M] added. As a result, the intensity of the fluorescence emission was reduced which was shown figure.3.The outcome was approximated using the Stern-Volmer equation and indicates that complexes may bind to CT-DNA and replace EB from DNA. This further indicates the intercalation of the complexes to CT-DNA. Stern-volmer equation used to calculate the results.  $K_{sv}$  value is obtained from the linear fit plot of  $I_0/I$  versus [complex]/[DNA] is  $1.65 \times 10^4 \, \text{M}^{-1}$  obtained.

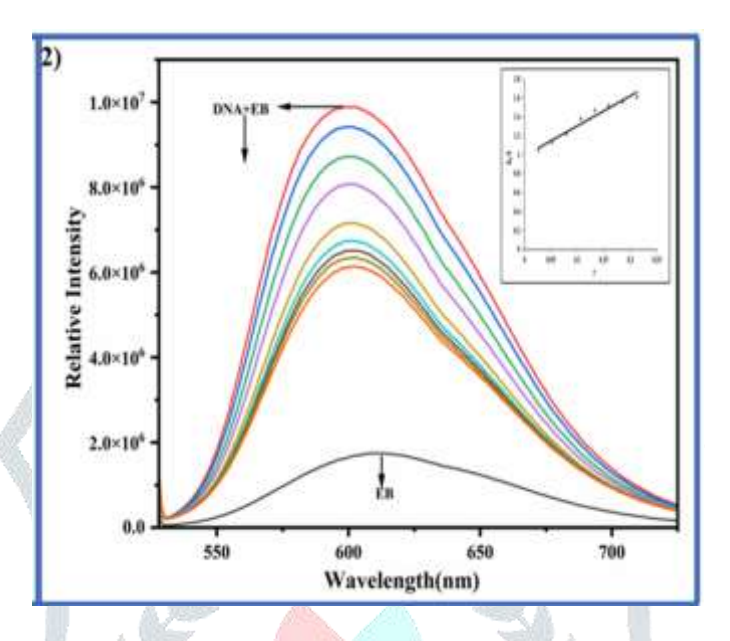


Fig.3.Fluorescence quenching studies of DNA-EB complex (DNA [130 mM] & EB [40 mM]) system, with the addition of complex arrow shows the decreasing emission intensity by increasing the concentration of complex [10-100 mM]. Inset: I<sub>0</sub>/I versus r.

#### 3.2.4. Light switch on experiment

Further to know the binding and emission property of complexes this experiment performed. In the presence of CT-DNA Further to know the binding and emission property of complexes this experiment performed. In the presence of CT-DNA light switch on and off behavior of the complexes monitored which was shown in figure.4. The luminescence behavior of the complexes altered by the addition of Co<sup>+2</sup> and followed by addition of EDTA. The emission intensity was high when the complex bound to CT-DNA (switch on), whereas Co<sup>2+</sup> (0.02 mM) quenches the emission of the DNA-bound complex, turning off the light. To this solution when EDTA added then emission intensity of the complex again regained (Light switch on). This suggests that the creation of the EDTA–Co<sup>2+</sup> strong combination releases the heterometalic complex (Co<sup>2+</sup>–complex 1) once more (Liu, 2010). The complex has shown same kind of luminescent behavior, which is altered by the DNA-bound complex's altered luminescence when Co<sup>2+</sup> and EDTA are present indicates how medication therapy is modulated by it.

#### 3.2.5. Viscosity studies

Viscosity studies conducted to find out the mode of binding of the metal complex to CT-DNA. Hydrodynamic experiments are crucial to understand the length change and stiffening of the rod-like DNA by inserting ligand between neighboring base pairs of DNA in solution in the absence of crystallographic data. Intercalating ligands, intercaltes in between the base pairs of DNA which lengthens the double helix and by increases the viscosity of DNA solution. Classical intercalation binding model shows increased viscosity of DNA by lengthening of DNA helix due to the separation of double helix to accommodate the ligand in between the base pairs (Chaires, 1997). The best example for classical intercalation binding mode was observed in EtBr. In this study, increased concentrations of metal complexes were added to the CT-DNA, an extension in the DNA length there by increased viscosity observed.

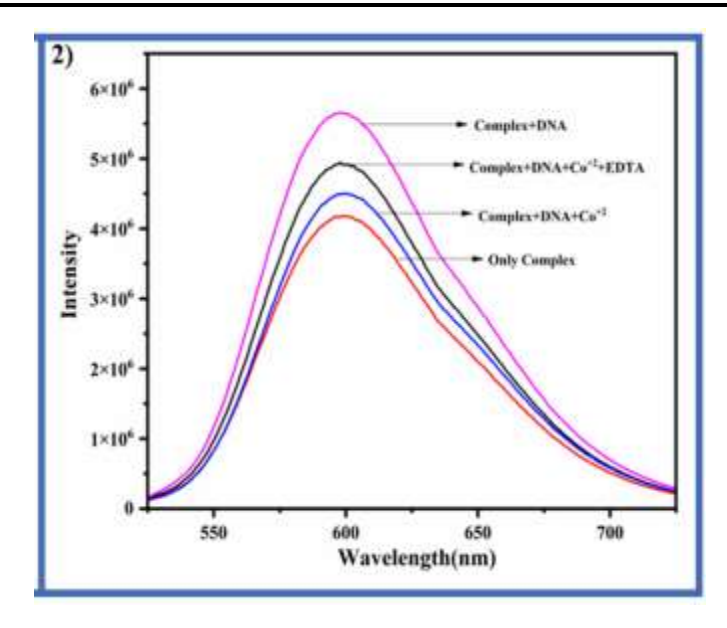


**Fig.4.**DNA light switch on and off experiment of complex showing the emission changes upon the addition of DNA (Switch on),  $Co^{2+}$  (Switch off) and EDTA (Switch on) to the complexes.

Further on comparison with EtBr an intercalating ligand, as shown in the figure.5 the results of the complex binding in between the base pairs of DNA which supports intercalation binding mode. The results from this study strongly supported by observations from electronic spectroscopy and fluorescence emission.

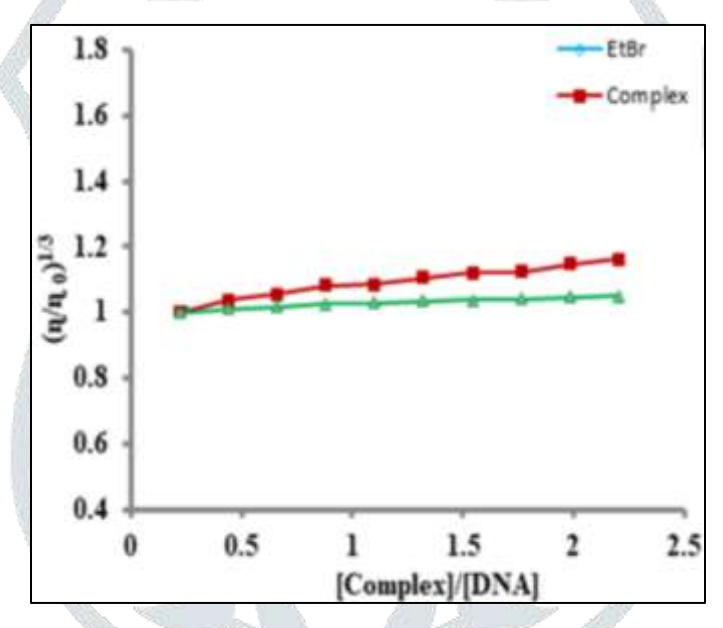


**Fig.5.** Viscosity study of complex in Tris-HCl buffer with increasing amounts of complex and EtBr on the relative viscosity of CT-DNA at room temperature.

#### 3.2.6. Photo cleavage

Using pBR322 DNA, nuclear activity of the Ru (II) complex was measured using agarose gel electrophoresis. Plasmid DNA become electrophoresis, a reasonably quick process. When the supercoiled shape is intact, migration is seen in form I. If nicking, or scission on a single strand, happens, then a slower-moving, open circular form (form II) will result from the supercoiled form relaxing. When both threads are split, a linear form known as form III moves. This form is migrates in between I and II. Photo cleavage experiment was performed by taking pBr322 which was incubated along with the complex  $(20\mu M)$  and irradiated for 60 min at 365nm under UV light continuously. When the metal complex was absent no signs of DNA cleavage shown in lane.1. Once the amount of Ru(II) complex was added, the equivalent of form I progressively dropped, while the quantity of type II enhanced, as Fig.6 illustrates.

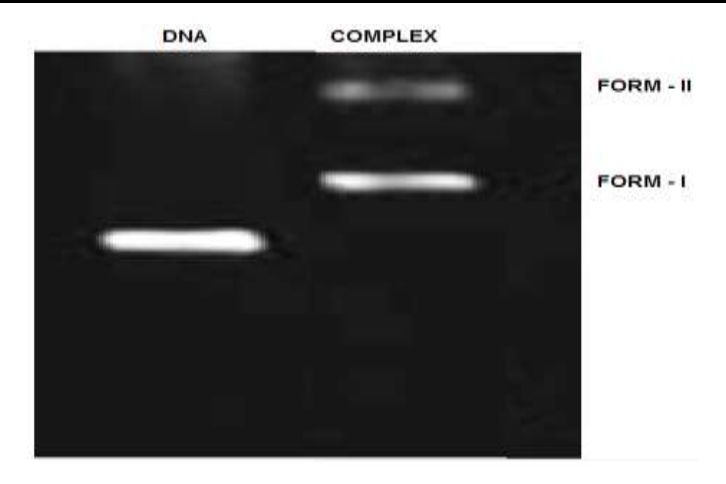


Fig.6 Photo activated cleavage [Ru(phen)<sub>2</sub>TMPIP]<sup>+2</sup> complex with the concentration range of 20 μM.

# 3.3. Cytotoxicity

The MTT method was used to evaluate the antiproliferative activities of the Ru (II) complexes again MCF-7 (Human breast cancer), comparison with- Doxorubicin as positive control. The Ru(II) polypyridyl complex displays excellent antitumor activity towards the selected cancer cell line. Ru(II) complex exhibited well activity against MCF-7 cells with  $IC_{50} = 17.42 \pm 029 \mu g/ml$  and standard doxorubicin  $IC_{50} = 3.66 \pm 0.07 \mu g/ml$ . Cell viability of MCF-7 is more in case of complex because of the presence of phenanthroline ligand shown in the figure .7. Thus, this complex exhibit high inhibitory effect on the cell growth in MCF-7 cell line and may be used as a potent anticancer drugs against breast cancer.

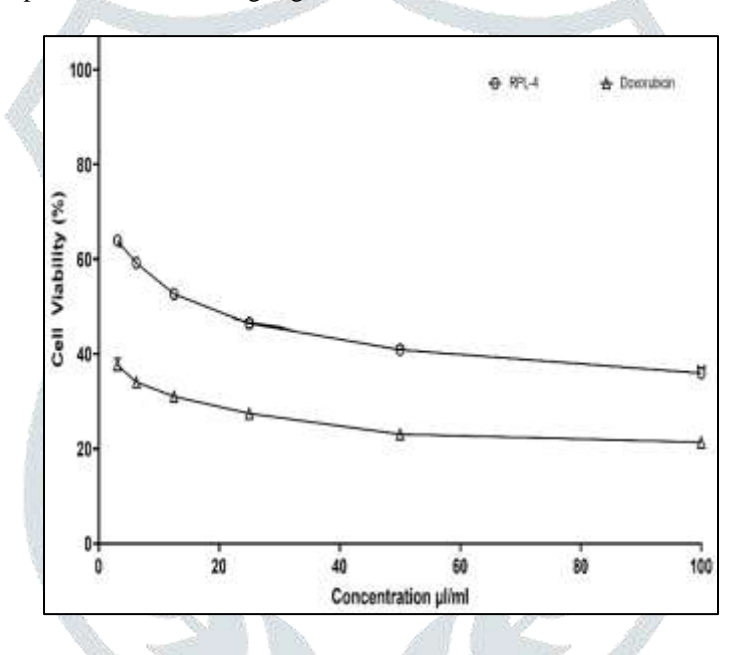


Fig.7.Cell viability of MCF-7 cell line in vitro treatment with complexes  $[Ru (phen)_2(TMPIP)]^{2+}$ . Every data point is the average  $\pm$  standard error derived from a minimum of three separate experiments.

#### 3. Conclusion

The *invitro* cytotoxicity of ruthenium (II) polypyridyl complex with novel intercalator ligand (TMPIP) has been estimated to show promising anticancer activity against cell line MCF-7. The metal complex auxiliary ligand is crucial in controlling the activity. The DNA binding studies of the Ru (II) complex examined by UV–Vis absorption, fluorescence quenching titrations and viscosity measurements which concluded that the binding mode of complex against DNA is an intercalative mode. The above data showed that the complex  $(K_b = 1.5 \times 10^5 M^{-1})$  bind to DNA effectively. In the absence of DNA, the complexes were efficiently quenched by the quencher. Subsequent investigations into photolytic cleavage of supercoiled pBR322 DNA in the presence of UV light demonstrated that the novel Ru (II) polypyridyl complex exhibit a strong DNA cleavage activity (photo cleavage). It is found that ruthenium compounds with the 1, 10 phenanthroline ligand has potent cancer-cell inhibition and Ancillary ligand's function is to ensure its uniqueness in DNA binding. It's interesting to note that the complex control a comparable arrangement of characteristics, suggesting that they may share an apoptosis induction mechanism

**Acknowledgement** - The authors GS and NN are thankful to The Head, Department of Chemistry and the Principal, University College of Science, Saifabad, Osmania University, and The Head, Department of Chemistry and the Principal, University College

of Science, Tarnaka, Osmania University, Hyderabad for the facilities to carry out this work. The Authors are thankful to the DST FIST, New Delhi for facility of the Computational Lab at Department of Chemistry, University College of Science, Saifabad, Osmania University.

Conflict of Interest- On behalf of all authors, the corresponding author states that there is no conflict of interest

#### References

- [1].Guang-Bin Jiang, Wen-Yao Zhang, Miao He, Yi-Ying Gu, Lan Bai, Yang-Jie Wang, Qiao Yan Yi, Fan Du, Development of four ruthenium polypyridyl complexes as antitumor agents: Design, biological evaluation and mechanism investigation. J InorgBiochem 2020 https://doi.org/10.1016/j.jinorgbio.2020.111104
- [2] A. Nataro, G. Gasser, 2017. Monomeric and dimeric coordinatively saturated and substitutionally inert Ru (II) polypyridyl complexes as anticancer drug candidates, Chem. Soc. Rev. 46 (2017) 7317e7337.
- [3] K. Hu, F. Li, Z. Zhang, F. Liang, 2017. Synthesis of two potential anticancer copper (II) complex drugs: their crystal structure, human serum albumin DNA binding and anticancer mechanism, New J. Chem. 41: 2062e2072.
- [4] L.R. Kelland, N.P. Farell, S. Spinelli, in Uses of Inorganic Chemistry in Medicine, ed. N. P. Farrell, RSC, Cambridge, 1999, 109.
- [5] Oun, R.; Moussa, Y.E.; Wheate, N.J. The side effects of platinum-based chemotherapy drugs: A review for chemists. *Dalton Trans.* **2018**, *47*, 6645–6653.
- [6] Kuhn PS, Pichler V, Roller A, Hejl M, Jakupec MA, Kandioller W, et al. Improved reaction conditions for the synthesis of new NKP-1339 deriva-tives and preliminary investigations on their anticancer potential. Dalton Trans. 2015;44(2):659–68.
- [7]Lentz F, Drescher A, Lindauer A, Henke M, Hilger RA, Hartinger CG, et al. Pharmacokinetics of a novel anticancer ruthenium complex (KP1019, FFC14A) in a phase I dose-escalation study. Anticancer Drugs. 2009;20(2):97–103.
- [8] Yulin Yang, Guojian Liao and Chen Fu \* Recent Advances on Octahedral Polypyridyl Ruthenium(II) Complexes as Antimicrobial Agents, Polymers 2018, 10, 650; doi:10.3390/polym10060650
- [9] Novakova O, Kasparkova J, Bursova V, Hofr C, Vojtiskova M, Chen HM, et al. Conformation of DNA modified by monofunctional Ru(II) arene complexes: recognition by DNA binding proteins and repair. Relationship to cytotoxicity. Chem Biol. 2005;12(1):121–9.
- [10]. Morrall, J.P., Humphrey, M.G., Dalton, G.T., Cifuentes, M.P., Samoc, M. (2006). NLO Properties of Metal Alkynyl and Related Complexes. In: Papadopoulos, M.G., Sadlej, A.J., Leszczynski, J. (eds) Non-Linear Optical Properties of Matter. Challenges and Advances in Computational Chemistry and Physics, vol 1. Springer, Dordrecht. <a href="https://doi.org/10.1007/1-4020-4850-5\_17">https://doi.org/10.1007/1-4020-4850-5\_17</a>
- [11]. Jabłońska-Wawrzycka A, Rogala P, Michałkiewicz S, et al. Ruthenium complexes in different oxidation states: synthesis, crystal structure, spectra and redox properties. Dalton Trans. 2013;42(17):6092–6101. doi:10.1039/c3dt32214a
- [12]. Strasser S, Pump E, Fischer R, et al. On the chloride lability in electron-rich second-generation ruthenium benzylidene complexes. Monatsh Chem. 2015;146(7):1143–1151. doi:10.1007/s00706-015-1484-x
- [13]. Norden, B.; Lincoln, P.; Akerman, B.; Tuite, E. DNA interactions with substitution-inert transition metal ion complexes. Metal Ions Biol. Syst. 1996, 33, 177–252.
- [14] Luedtke, N.W.; Hwang, J.S.; Nava, E.; Gut, D.; Kol, M.; Tor, Y. The DNA and rna specificity of eilatinru(ii) complexes as compared to eilatin and ethidium bromide. Nucleic Acids Res. 2003, 31, 5732–5740.
- [15] Metcalfe, C.; Thomas, J.A. Kinetically inert transition metal complexes that reversibly bind to DNA. Chem. Soc. Rev. 2003, 32, 215–224.
- [16] Ang WH, Casini A, Sava G, Dyson PJ. Organometallic ruthenium-based antitumor compounds with novel modes of action. J Organomet Chem. 2011;696(5):989–98.
- [17] Schatzschneider U, Niesel J, Ott I, Gust R, Alborzinia H, Wolf S (2008) Cellular uptake, cytotoxicity, and metabolic profiling of human cancer cells treated with ruthenium(II) polypyridyl complexes [Ru(bpy)2(N-N)]Cl2 with N-N=bpy, phen, dpq, dppz, and dppn. Chem Med Chem 3:1104-1109
- [18] Tan CP, Liu J, Chen LM, Shi S, Ji LN (2008) Synthesis, structural characteristics, DNA binding properties and cytotoxicity studies of a series of Ru(III) complexes. J InorgBiochem 102:1644–1653
- [19] Puckett CA, Barton JK (2008) Mechanism of cellular uptake of a ruthenium polypyridyl complex. Biochemistry 47:11711–11716.
- [20] Yamada M, Tanaka Y, Yoshimoto Y, Kuroda S, Shimao I (1992) Synthesis and properties of diaminosubstistuted di pyrido [3,4-a:2', 3'-c] phenazine. Bull ChemSocJpn 65:2007–2009
- [21]. B. P. Sullivan, D. J. Salmon, T. Meyer, Inorg. Chem. 1978, 17, 3334.

- [22]. Navaneetha Nambigari\*, ArunaKodipaka, Ravi Kumar Vuradi, Praveen Kumar Airva and Satyanarayana Sirasani. 2022. Binding and Photocleavage studies of Ru (II) Polypyridyl Complexes with DNA: An In Silico and Antibacterial activity. Analytical Chemistry Letters. 12 (2), 266 282. http://doi.org/10.1080/22297928.20211110.
- [23].Navaneetha Nambigari,Aruna Kodipaka·Ravi Kumar Vuradi·Praveen Kumar Airva· Satyanarayana Sirasani. A Biophysical Study of Ru(II) Polypyridyl Complex, Properties and its Interaction with DNA. Journal of Fluorescence. https://doi.org/10.1007/s10895-021-02879-x
- [24]. Aveli Rambabu, Marri Pradeep Kumar, Nirmala Ganji, SreenuDaravath & Shivaraj, Journal of Biomolecular Structure and Dynamics, DOI: 10.1080/07391102.2019.1571945
- [25]. Ravi Kumar Vuradi, **Navaneetha Nambigari**, Pushpanjali Pendyala, Srinivas Gopu, Kotha Laxma Reddy, G. Deepika, M. Vinoda Rani and Satyanarayana S\*. 2020. Study of Anti-Apoptotic mechanism of Ruthenium(II) Polypyridyl Complexes via RT-PCR and DNA binding. Applied Organometallic Chemistry. 34:3, e5332. [IF 3.14]. ISSN:1099-0739. https://doi.org/10.1002/aoc.5332
- [26] Zheng, R.H., Guo, H.C., Jiang, H.J., Xu, K.H., Liu, B.B., Sun, W.L., Shen, Z.Q. (2010). A new and convenient synthesis of phendiones oxidated by KBrO3 /H2 SO4 at room temperature. Chinese Chem. Lett. 21(11): 1270-1272
- [27].Goss, C.A., Abruna, H.D. (1985). Spectral, electrochemical and electrocatalytic properties of 1,10-phenanthroline-5,6-dione complexes of transition metals. Inorg. Chem. 24(25): 4263-4267.
- [28]. Liu, X.W., Shen, Y.M., Lu, J.L., Chen, Y.D., Li, L., Zhang, D.S. (2010). Synthesis, DNA-binding and photocleavage of "light switch" complexes [Ru(bpy)2 (pyip)]2+ and [Ru(phen)2 (pyip)]2+. Spectrochim. Acta A Mol. Biomol. Spectrosc. 77: 522-527.
- [29]. Chaires, J.B. (1997). Energetics of drugDNA interactions. Biopolymers. 44(3): 201-215.
- [30]. [E. A. Steck, A. R. Day, J. Am. Chem. Soc. 1943, 65, 452

